Collective Behavior of Antagonistically Acting Kinesin-1 Motors

Cecile Leduc,[1,2] Nenad Pavin,[3,4] Frank Jülicher,[3,*] and Stefan Diez[1,†]

[1]*Max Planck Institute of Molecular Cell Biology and Genetics, Dresden 01307, Germany*
[2]*Centre de Physique Moleculaire Optique et Hertzienne, CNRS-Universite Bordeaux 1, Talence, France*
[3]*Max Planck Institute for the Physics of Complex Systems, Dresden 01187, Germany*
[4]*Department of Physics, Faculty of Science, University of Zagreb, Zagreb 10002, Croatia*

(Received 1 February 2010; published 17 September 2010)

In many subcellular force-generating systems, groups of motor proteins act antagonistically. Here, we present an experimental study of the tug of war between superprocessive kinesin-1 motors acting on antiparallel microtubule doublets *in vitro*. We found distinct modes of slow and fast movements, as well as sharp transitions between these modes and regions of coexistence. We compare our experimental results to a quantitative theory based on the physical properties of individual motors. Our results show that mechanical interactions between motors can collectively generate coexisting transport regimes with distinct velocities.

DOI: 10.1103/PhysRevLett.105.128103 PACS numbers: 87.16.Uv, 87.16.A−, 87.16.Nn

Active transport and force generation, mediated by the collective operation of cytoskeletal motor proteins, is essential to build and maintain the spatial organization in living cells. Collective behaviors of motors were first addressed theoretically, predicting dynamic transitions where the velocity of movement changes abruptly [1–3]. Recently, a number of subcellular force-generating systems have been studied by a combination of theory and experiments [4–7]. In these studies, novel behaviors including stop-and-go and bidirectional movement were reported *in vitro* and *in vivo* [8–11]. Among the underlying principles for bidirectional cargo transport is the tug of war, where antagonistic motors work simultaneously by exerting force in opposite directions [3,8,12,13]. The tug-of-war scenario is also important for subcellular processes such as mitosis [9,14] and nuclear [5] and spindle [15] oscillations, as well as axonemal motility [6].

Here, by a combination of *in vitro* experiments and theory, we quantitatively characterize the collective dynamics of antagonistic motors. In particular, we realized an antagonistic arrangement of motors by generating antiparallel microtubule doublets and studied their movement in gliding motility assays on surfaces coated with high densities of kinesin-1 [16] (Fig. 1). In this geometry, the lengths of the microtubules (MTs) in the doublet determine the numbers of motors that are available for force generation in both directions. Our setup allows us to use a single type of motor which has been well characterized on the level of single molecules [17]. In order to identify the key mechanisms underlying the collective behaviors of antagonistic motors, we developed a theory based on the physical properties of individual motors. We show that it is essential to include the finite stiffness of the motors [15], in addition to the nonlinear force-velocity relationship and the load-dependent detachment rate of single motors [13].

Stabilized MTs of fixed lengths ranging from 5 to 15 μm were prepared by *in vitro* polymerization. MT doublets were formed by incubation with anti-β-tubulin antibodies which possess two tubulin binding sites [Fig. 1(a)]. In order to distinguish parallel from antiparallel doublets, we employed two-color polarity marking of MTs. Alexa-488 labeled MT seeds were created and subsequently subjected to a mixture of Alexa-488 and Rhodamin-labeled tubulin for MT elongation (see Methods in [18]). MT extensions predominantly grew at the plus ends, resulting in uniformly labeled green MTs with additional red signals at the plus ends. This procedure allowed us (i) to unambiguously determine the MT polarities in the doublets, (ii) to precisely measure the MT lengths, and (iii) to count the number of cross-linked MTs from the fluorescent signals [Figs. 1(b) and 1(c) and [18]]. At high motor density (about 500 kinesins/μm^2), when fluctuations of the number of active motors are expected to be small compared to the number of available motors, the antiparallel MT doublets

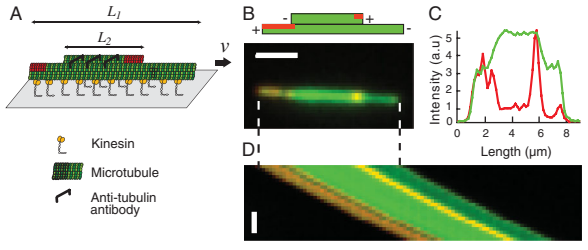

FIG. 1 (color). Gliding motility assay of antiparallel polarity-marked MT doublets. (a) Schematic diagram of MT doublets with individual MT lengths L_1 and L_2 and gliding velocity v. (b) Schematic and dual-color epifluorescence image of an antiparallel doublet; bar 2 μm. (c) Fluorescence intensity profiles in the red and the green channels. (d) Kymograph illustrating the doublet movement; vertical scale bar, 1 min.

adopted a unidirectional movement with a constant velocity and with the direction determined by the longer (or "leading") MT. In the following, the leading MT is characterized by length L_1 and the trailing MT by length L_2. We systematically analyzed the doublet velocities as a function of the relative difference of MT lengths $\Delta\ell = (L_1 - L_2)/(L_1 + L_2)$ for 56 antiparallel doublets [Figs. 2(a) and 2(b)]. At 1 mM ATP concentration [Fig. 2(a)], the movement was either slow ($v/v_0 \lesssim 0.2$) or fast ($v/v_0 \gtrsim 0.85$), where v_0 is the gliding velocity of a single MT. For a range of $\Delta\ell$, two values of the velocity coexisted. A sharp switchlike transition from the branch of slow movement to the branch of fast movement was observed for increasing $\Delta\ell$. Such discontinuous behavior and a coexistence region are characteristic for a first-order phase transition. A sharp transition was also observed for smaller gliding velocities v_0 [at 10 μM ATP, Fig. 2(b)]. However, the position of the transition was shifted towards larger $\Delta\ell$, and the width of the coexistence region was reduced.

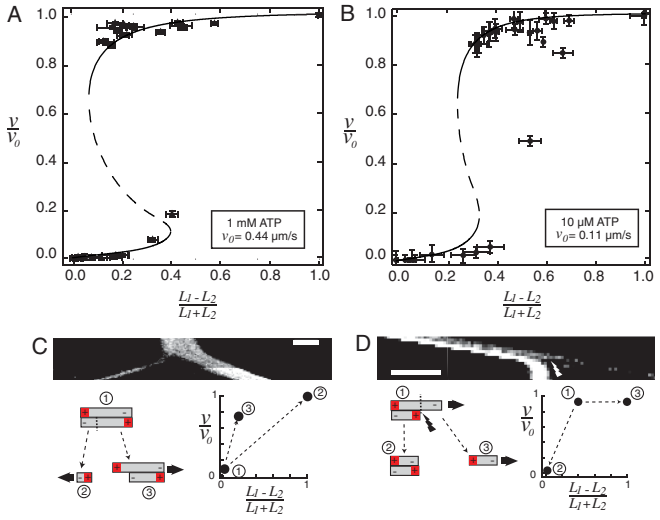

FIG. 2 (color). Gliding velocities of antiparallel MT doublets. (a) Experimental values (black triangles) of normalized doublet velocities v/v_0 as a function of the relative MT length differences $\Delta\ell = (L_1 - L_2)/(L_1 + L_2)$ at saturating ATP concentration (1 mM ATP, $v_0 = 0.44 \pm 0.07$ μm/s, mean $\pm$ SD, $n = 28$ from 6 experiments). (b) Experimental values (black circles) of normalized doublet velocities at reduced ATP concentration (10 μM ATP, $v_0 = 0.12 \pm 0.04$ μm/s, $n = 28$ from 6 experiments). Error bars display the experimental uncertainties. The lines shown in (a) and (b) represent the most accurate results of our theoretical description to the experimental data using the nonlinear force-velocity relationship of individual motors from Ref. [25] (see [18], Discussion). (c) Kymograph of doublet movement undergoing a transition from slow to fast movement (bar 2 μm, total time 126 s) and (d) from fast to slow movement (bar 2 μm, total time 70 s). Schematic drawings of the transition induced by spontaneous MT breakage within the doublet (c) and by laser cutting indicated by a flash (d) are depicted together with the resulting velocity changes. The increase in fluorescence intensity observed after about 1 min in (c) originates from a manual increase of the imaging gain.

To investigate if transitions between slow and fast movement could be triggered on the level of individual doublets, we studied events where the lengths of MTs changed suddenly. We observed that doublets, which originally had a slow movement due to both MTs having about the same length, rapidly adopted a fast movement by spontaneously losing a small portion of one of the MTs [Fig. 2(c)]. We also found that fast doublets could be stopped when the length of the longer MT was reduced by laser cutting [Fig. 2(d); see [18] for further examples]. From these results, we conclude that direct transitions between the slow and the fast branch can be induced by changes in filament length. This finding also rules out the possibility that fast doublet motion occurs because the trailing MT is simply "carried" by the leading MT while itself not interacting with the kinesin-1 motors.

In order to quantitatively understand the underlying principles of our experimental results, we developed a theoretical description for the movement of antiparallel MT doublets [Fig. 3(a)]. Motors are characterized by a force-velocity relation $v_m(f)$, where v_m is the velocity of motion along a MT towards the plus end and f denotes the load force on an individual motor ($f > 0$ corresponds to a force in the minus direction). Motors are attached to a substrate by elastic linkers of stiffness k ("motor stiffness") [15]. We consider the left and right MTs separately. For the left MT, the load force exerted by the elastic linker is $f = ky$, where y is the linker extension. If the MT moves relative to the substrate with velocity v, this extension changes as $dy/dt = v + v_m(f)$. We now define the probability density $p_a(y, t)$ for a motor with linker extension y to be attached to the left MT. Likewise, the probability density for a motor to be detached is denoted $p_d(y, t)$. The attachment probability obeys

$$\partial_t p_a = -\partial_y \left[\frac{dy}{dt} p_a \right] + \omega_{\text{on}} p_d - \omega_{\text{off}} p_a, \tag{1}$$

where ω_{on} and ω_{off} are the motor attachment and detachment rates, respectively. A key ingredient of our theory is the fact that the detachment rate ω_{off} depends on the load force experienced by a single motor [19–22]:

$$\omega_{\text{off}}(y) = \omega_0 \exp(k|y|/f_c), \tag{2}$$

where ω_0 is the detachment rate in the absence of load and f_c is a characteristic detachment force. If the rate of linker relaxation for a detaching motor is fast compared to the rate of attachment, the distribution of detached motors relaxes to [15]

$$p_d(y, t) = Q_d(t) A \exp\left(-\frac{ky^2}{2k_B T} \right), \tag{3}$$

where $Q_d(t) = \int_{-\infty}^{\infty} p_d(y, t) dy$ is the probability for a motor to be detached and $A = [k/(2\pi k_B T)]^{1/2}$.

In the steady state, $\partial_t p_a = 0$, $\partial_t p_d = 0$, and the doublet velocity v is constant. The average force exerted by a single motor on the left MT is then given by $\bar{f}_2(v) = \bar{f}(v)$, where $\bar{f}(v) = -k \int_{-\infty}^{\infty} y p_a dy$. The total force on

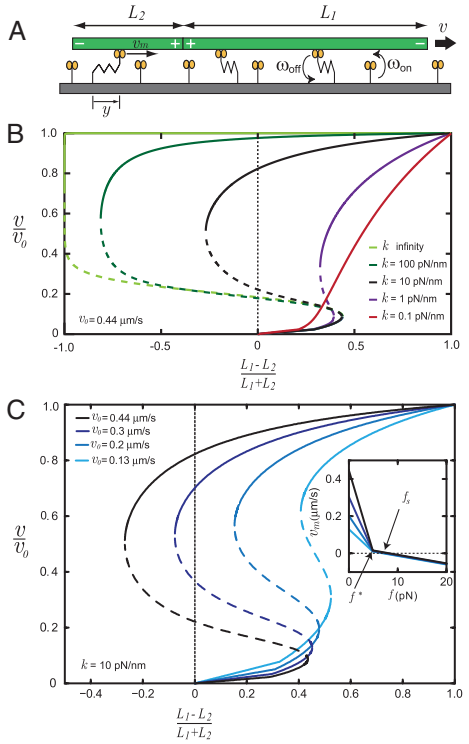

FIG. 3 (color). Theoretical results. (a) Schematic representation of the one-dimensional model. The MT doublet is represented by two MTs joined at their plus ends. The lengths of the left and right MTs are denoted L_2 and L_1, respectively, in consistence with the annotations in Figs. 1 and 2. (b) Normalized doublet velocities v/v_0 as functions of the relative MT length differences for different values of motor stiffness k [where $v_0 = 0.44$ μm/s is the load free single motor velocity $v_m(0)$]. The other parameter values were either taken from previous studies ($\omega_{on} = 5\ s^{-1}$, $f_c = 3$ pN [22], $f_s = 7$ pN [31]) or measured here ($\omega_0 = 0.01\ s^{-1}$, which we note is an unexpectedly low detachment rate for the kinesin-1 construct used in this work; however, we consistently obtained this value in multiple measurements under our experimental conditions—see also [18]). The solid lines correspond to locally stable steady states for which the slope $dv/d\Delta\ell > 0$. Broken lines indicate unstable states with negative slope $dv/d\Delta\ell < 0$. The force-velocity relation used is shown as an inset in (c). (c) Normalized doublet velocities for different values of v_0 [with $k = 10$ pN/nm; other parameter values as in (b)]. Inset: The force-velocity relation of individual motors is described for simplicity by a piecewise linear function $v_m(f) = v_0 - [v_0 + \alpha(f^* - f_s)]f/f^*$ for $f \le f^*$ and $v_m(f) = -\alpha(f - f_s)$ for $f > f^*$. Parameters are $f^* = 5$ pN and $\alpha = 5 \times 10^3$ m/(Ns) evaluated from Ref. [17].

the left MT is thus $F_2 = n_0 L_2 \bar{f}_2(v)$, where n_0 denotes the linear density of motors that can attach to the MT. Accounting for the opposite orientation of left and right MTs, the average force exerted by a single motor on the right MT is $\bar{f}_1(v) = -\bar{f}_2(-v) = -\bar{f}(-v)$. The total force on the right MT is $F_1 = n_0 L_1 \bar{f}_1(v)$, and, by neglecting viscous friction acting on the doublet [23], the force balance reads

$$L_2 \bar{f}(v) - L_1 \bar{f}(-v) = 0. \quad (4)$$

From Eq. (4), the doublet velocity can be determined as a function of the ratio of the MT lengths L_1/L_2 and thus of $\Delta\ell = (L_1/L_2 - 1)/(L_1/L_2 + 1)$.

Normalized doublet velocities, obtained from numerical solutions to Eq. (4) (see [18]), are shown in Figs. 3(b) and 3(c) for a simple choice of a piecewise linear force-velocity relation [see inset in Fig. 3(c)]. We first investigated the role of the motor stiffness k, which is the least known parameter, and its influence has often been neglected in previous studies [Fig. 3(b)]. In all cases, except for small k (below 1 pN/nm), two stable branches, corresponding to slow and fast movement, exist. In both velocity regimes, the doublet velocity increases with an increase in $\Delta\ell$. For small $\Delta\ell$, the longer MT is leading and slow movement occurs with $v \ll v_0$. Here $dv/d\Delta\ell \simeq \alpha f_s/v_0$, with α characterizing the load dependence of the single motor velocity at the stall force. For large $k > 1$ pN/nm, fast movement with velocities $v \simeq v_0$ occur for a wide range of $\Delta\ell$, and, for certain values of $\Delta\ell$, both slow and fast movement coexist. For $k \gg 1000$ pN/nm, a change in the motor stiffness no longer influences the doublet velocity curves. For decreasing values of k, the slope $dv/d\Delta\ell$ of the fast branch increases while the width of the coexistence region decreases. We also investigated the influence of the single motor velocity v_0 on the doublet velocity curve [Fig. 3(c)]. In agreement with our experimental data, the range of $\Delta\ell$ for coexistence is reduced as the velocity v_0 decreases. Note that in all our theoretical results the presence of the coexistence region in the doublet velocity curves is a robust result of our theory over a wide range of parameters (see [18] for variations of ω_0, ω_{on}, and f_c).

Beyond the equations presented above, we interpret the slow and the fast motility regimes as follows: On the slow branch, motor attachment is faster than motor detachment for both MTs (see [18]). Therefore, motors are dominantly attached to the MTs. The difference in the number of motors attached to the left and right MTs is then proportional to the difference of MT lengths. Thus, the doublet velocities are slow for small $\Delta\ell$. On the fast moving branch, motors detach rapidly from the trailing MT (see [18]) because they experience superstall load forces while motors on the leading MT remain attached. Therefore, the fraction of attached motors on the leading MT is much higher than that on the trailing MT, and the doublet velocity can reach values close to v_0.

Our work shows that the load-dependent detachment is essential for the existence of the two observed branches of motility. Load-dependent detachment of infinitely stiff motors has been shown to suffice to capture key features of different biological processes like membrane tube formation, spindle [15], and chromosome [24], or meiotic nuclear [5] oscillations, as well as stochastic bidirectional cargo transport [13]. However, we find here that the motor stiffness k is also a key parameter. The doublet velocities observed in our experiments at both high and low ATP could be reliably predicted for a unique set of parameters only when taking into account the finite stiffness of the

molecular motors. Using a simplified piecewise linear force-velocity relationship for individual motors, we found that a motor stiffness of $k = 10$ pN/nm provides the best agreement between experiment and theory. This choice generates the appropriate slopes of the stable branches [compare the black curve in Fig. 3(b) with Fig. 2(a)] and can account for the changes of the doublet velocity curve due to changes in ATP concentration, which are described by changes of v_0 [compare Fig. 3(c) with Figs. 2(a) and 2(b)]. We note, however, that for $k = 10$ pN/nm the region of coexistence is larger than the one observed experimentally. We find that this difference disappears when we use a more complex, nonlinear, force-velocity relation based on a two-state stochastic model [25] [see lines in Figs. 2(a) and 2(b)]. This force-velocity relation quantitatively describes the single-kinesin-1 experiments reported in Ref. [17] but involves more parameters than the simpler piecewise linear relation (see [18]). Using this nonlinear force-velocity relation we estimate a motor stiffness $k \simeq 2$ pN/nm. We can only speculate about the origin of the remaining discrepancy between this value and earlier estimates ($k \simeq 0.5$ pN/nm [26,27]). The difference could arise because of different assay conditions such as different methods of motor attachment to the surface. It is interesting to note that such a difference could also result from non-Hookian effects in the motor elasticity. In our model, such effects do not change the main results.

The pronounced sensitivity of the doublet velocity to the shape of the force-velocity relation suggests that nonlinearities in the mechanical properties of individual motors are emphasized in the collective motion of many motors. Therefore, our results provide an example for inferring certain physical properties of single molecules, like the negative velocity region (superstall force), by examining the behavior of many molecules acting collectively.

We have developed a novel assay based on antiparallel filament doublets to mimic the forces of antagonistic motors *in vitro*. Although experimentally more challenging, this assay can be extended towards scenarios where motors are softly coupled to their substrate, resembling vesicular transport, as well as where motors interact with dynamic MTs, resembling force generation in the mitotic or meiotic spindle. However, already in the geometry reported here, it will be interesting and straightforward to investigate motors of different processivities [28] (such as kinesin-1 under varied buffer conditions or nonprocessive kinesin-14, myosin-II, and axonemal dynein), motors of different directionality [8], or motors of the same directionality but with different velocities [29,30]. These behaviors, which play an important role in a number of cellular processes, naturally emerge in systems where motors operate antagonistically.

The authors thank J. Howard for stimulating discussions, B. Nitzsche, T. Korten, C. Braeuer, and the MPI-CBG light microscopy facility for experimental help, and A. Jimenez-Dalmaroni for early participation in the theoretical analysis, as well as S. Grill, V. Krstic, and I. Tolic-Norrelykke for critical reading of the manuscript. This work has been financially supported by the BMBF (03N8712), the DFG (DI 1226/3), and the Max Planck Society.

*julicher@pks.mpg.de
†diez@mpi-cbg.de

[1] F. Jülicher and J. Prost, Phys. Rev. Lett. **75**, 2618 (1995).
[2] F. Jülicher, A. Ajdari, and J. Prost, Rev. Mod. Phys. **69**, 1269 (1997).
[3] M. Badoual, F. Jülicher, and J. Prost, Proc. Natl. Acad. Sci. U.S.A. **99**, 6696 (2002).
[4] T. Surrey *et al.*, Science **292**, 1167 (2001).
[5] S. K. Vogel *et al.*, PLoS Biol. **7**, e87 (2009).
[6] I. H. Riedel-Kruse *et al.*, HFSP J. **1**, 192 (2007).
[7] J. Howard, Annu. Rev. Biophys. **38**, 217 (2009).
[8] R. D. Vale, F. Malik, and D. Brown, J. Cell Biol. **119**, 1589 (1992).
[9] L. Tao *et al.*, Curr. Biol. **16**, 2293 (2006).
[10] V. Levi *et al.*, Biophys. J. **90**, 318 (2006).
[11] D. Riveline *et al.*, Eur. Biophys. J. **27**, 403 (1998).
[12] M. A. Welte, Curr. Biol. **14**, R525 (2004).
[13] M. J. Muller, S. Klumpp, and R. Lipowsky, Proc. Natl. Acad. Sci. U.S.A. **105**, 4609 (2008).
[14] G. Fink *et al.*, Nat. Cell Biol. **11**, 717 (2009).
[15] S. W. Grill, K. Kruse, and F. Jülicher, Phys. Rev. Lett. **94**, 108104 (2005).
[16] J. Howard, A. J. Hudspeth, and R. D. Vale, Nature (London) **342**, 154 (1989).
[17] N. J. Carter and R. A. Cross, Nature (London) **435**, 308 (2005).
[18] See supplementary material at http://link.aps.org/supplemental/10.1103/PhysRevLett.105.128103 for the methods and systematic controls.
[19] H. A. Kramers Physica (Utrecht) **7**, 284 (1940).
[20] A. Parmeggiani *et al.*, Europhys. Lett. **56**, 603 (2001).
[21] K. S. Thorn, J. A. Ubersax, and R. D. Vale, J. Cell Biol. **151**, 1093 (2000).
[22] M. J. Schnitzer, K. Visscher, and S. M. Block, Nat. Cell Biol. **2**, 718 (2000).
[23] A. J. Hunt, F. Gittes, and J. Howard, Biophys. J. **67**, 766 (1994).
[24] O. Campas and P. Sens, Phys. Rev. Lett. **97**, 128102 (2006).
[25] A. B. Kolomeisky and M. Fisher, Annu. Rev. Phys. Chem. **58**, 675 (2007).
[26] K. Kawaguchi, S. Uemura, and S. Ishiwata, Biophys. J. **84**, 1103 (2003).
[27] S. Jeney *et al.*, Chem. Phys. Chem. **5**, 1150 (2004).
[28] D. Hexner and Y. Kafri, Phys. Biol. **6**, 036016 (2009).
[29] X. Pan *et al.*, J. Cell Biol. **174**, 1035 (2006).
[30] A. G. Larson, E. C. Landahl, and S. E. Rice, Phys. Chem. Chem. Phys. **11**, 4890 (2009).
[31] S. M. Block *et al.*, Proc. Natl. Acad. Sci. U.S.A. **100**, 2351 (2003).